A Study of Crack Propagation in High-Density Polyethylene

RAY D. HOFFMAN, *United States Steel Corporation, Research Laboratory, Monroeville, Pennsylvania 15146*

Synopsis

In recent published work a method was proposed to calculate fracture toughness during the crack-propagation phase of the loading of notched specimens. In this paper, it is proposed that the fracture toughness J can have a value that does not exceed the product of the ultimate work to failure of the material, W_f, times a characteristic remaining ligament length b_m. It is proposed that crack propagation is unstable at ligament lengths less than b_m and does not, therefore, demand further strain–energy input. The fracture toughness J at any particular remaining ligament length b can be calculated from a term that is related to the area under the curve of the net section stress vs. the ratio of plastic load point displacement to remaining ligament length. Experimental data on the loading of double-edge-notched specimens of high-density polyethylene that were extended to failure were used to test the proposed theory. The experimental results were encouraging, although not conclusive, in supporting the proposed method of relating the crack toughness to the known material properties of the subject material.

INTRODUCTION

Recent developments in J-integral methods make it feasible to calculate the energies involved in crack opening and crack extension over the whole course of specimen failure for ductile materials.

The description that follows starts with the old, familiar linear elastic fracture case, cites the parallel, less known inelastic fracture case, then proceeds to the J-integral method as applied to crack propagation or tearing. The intended original contribution of this paper is to develop a limit or bound to the total energy of failure of a ductile specimen.

The J integral is developed in terms of the area under the load–displacement curve rather than the usual differential expression so that J may be calculated using data from a single specimen.

The tendency of a notched specimen to crack is related to the strain energy U introduced into the specimen by the displacement of the loading points (δ^t). Figure 1 indicates the specimen geometry. At a critical notch length, a crack initiates at the notch root. The critical value of the fracture toughness J (in Pa·m) is, for the linearly elastic fracture mechanics case,

$$J_{ic} = 2(U_0 - U)/ta \tag{1}$$

where

$$U = \int_0^{\delta^t} P d\delta^t = P\delta^t/2 \tag{2}$$

is the area under the load–displacement curve for linear elastic conditions; P is the load; a is the notch length; t is the specimen thickness; and U_0 is the area

Journal of Applied Polymer Science, Vol. 27, 2119–2130 (1982)
 CCC 0021-8995/82/062119-12$02.20

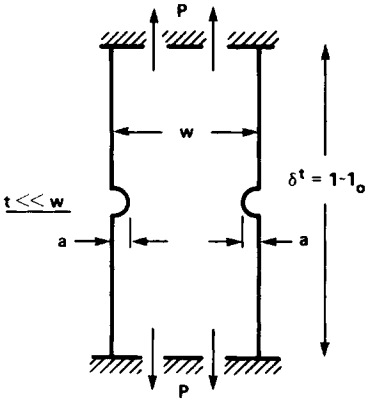

Fig. 1. Definition of parameters in notched specimens.

under the curve to the same δ^t for an unnotched specimen of otherwise identical geometry. The difference $(U_0 - U)$ is then just due to the presence of the notch.

The parallel inelastic case is that of a specimen very thin compared to its width and the distance between notch tips; the notch tips are blunt (i.e., the notch tip radius is of the same order of magnitude as the specimen thickness), and the material is ductile. On loading, crack initiation at the notch tip may be delayed until full yielding throughout the region of the notch plane has occurred. Furthermore, the notches are assumed sufficiently deep that the specimen in the regions away from the vicinity of the notch plane is in linear elastic strain. Under these conditions, the elastic portion of the load–displacement curve is small compared to the total displacement so that

$$U \cong P\delta^t \tag{3}$$

Under these conditions, the critical value of the fracture toughness J at crack initiation for a double-edge-notched specimen in tension is given by

$$J_{ic} = (2U - P\delta^t)/bt \tag{4}$$

where

$$b = W - 2a \tag{5}$$

W is the specimen width and a is the notch depth. If the elastic portion of the loading curve is significant, then

$$J_{ic} = G + (2U^p - P\delta^p)/bt \tag{6}$$

where G is the fracture toughness of the same material under linear elastic fracture mechanics conditions and the superscript P denotes use of the inelastic portion of the loading curve. The derivation of eq. (6) was first reported by Rice, Paris, and Merkel.[1] The secant area A of a load–total-displacement curve is given as [2]

$$2A = 2U^p - P\delta^p = 2U^t - P\delta^t \tag{7}$$

The secant area can be directly determined from either a load–total-displacement curve or a load–inelastic-displacement curve and can, therefore, be used to evaluate Eq. (6).

To obtain a perspective on the course of crack opening, initiation, and propagation, consider the following. When the load P is plotted as a function of the total load point displacement δ^t, as in Figure 2, a conventional load–elongation curve qualitatively identical to that obtained with an unnotched specimen is found. The initial slope is dependent on the notch depth, being given by

$$\text{initial slope} = E\left(1 + \frac{2\int Y^2 x dx}{l_0/W}\right)^{-1} (l_0/W)^{-1} \tag{8}$$

where E is Young's modulus, x is a reduced notch depth ($2a/W$), l_0 is the initial sample length, and Y is an empirical finite width correction factor given in terms of a polynomial in x.[3] If the notches are reasonably deep but $W \gg 2a$, the maximum load is related to the plane-strain yield strength (equal to $2\sqrt{3}$ times the uniaxial tension yield strength when the pressure coefficient of the yield surface is negligible and when a Von Mises yield condition applies).

As indicated schematically in Figure 2, changes in notch root radii change the position of the load–displacement curve at which cracks initiate at the notch root. The sharper the notch, the earlier the crack initiates. The load–displacement *after crack initiation* follows the dashed line appropriate to the root radii.

The course that the dashed line follows is not invariant but depends on two factors: the load train compliance (machine compliance plus compliance in the specimen away from the notch plane) and the processing or extensibility of the material in front of the extending crack. A crack is called "stable" if crack growth stops when the displacement of the load points stops. A crack is "unstable" if the crack proceeds to failure or complete separation even if the load-point displacement has ceased. Usually, "unstable" crack growth is very rapid—of the order of several meters per second. A complete characterization of the fracture toughness required to fracture completely a specimen requires an estimate of the energy required to propagate the growing cracks.

Recent work has extended the Rice, Paris, and Merkel work [Eq. (6)] to the situation of a propagating crack. Burns and McMeeking[4] obtained the result that

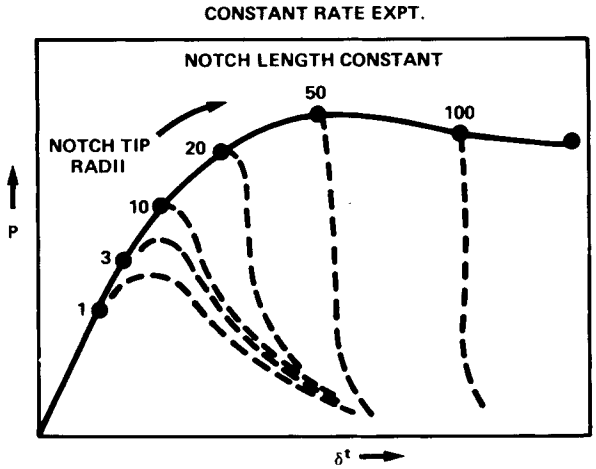

Fig. 2. Schematic diagram of a load–total-displacement curve of a notched specimen pulled in tension. Crack initiation depends on notch tip radius. The dashed lines represent the course of the load trace during the crack propagation phase.

$$J = G + b_1 \left[2 \int_0^{\delta_1^p / b_1} \frac{P}{tb} d\frac{\delta^p}{b} - \frac{P\delta_1^p}{tb_1^2} \right] \tag{9}$$

where b_1 is the ligament length after a given amount of crack growth has occurred. If no crack growth occurs, b remains constant through the test, and eq. (9) is identical with eq. (6). The Burns–McMeeking result applies to stable cracking only.

The quantity (P/tb) is seen to be an average net stress through the notch plane. The key plot to evaluate eq. (9) is a plot of (P/tb) vs. (δ^p/b). This plot will differ from Figure 2 in that δp is zero until yielding is fully developed through the notch plane or equivalently until after the maximum in Figure 2, and that the current notch plane cross-sectional area (tb) is being used. As the crack grows, the load will drop below the envelope curve of Figure 2, but the load drop is supposed to be compensated by the ligament length reduction to yield overlapping curves regardless of the starting ligament length. One of the experimental objectives is to check this point.

In Figure 3, a schematic is drawn by assuming that the plot of P/tb vs. δ^p/b encompasses a rectangular section. Assuming this relationship, the bracketed term of eq. (9) is simply $P\delta_1^p/b_1^2 t$ and $(J - G)$ is therefore $P\delta_1^p/b_1 t$. Although P/bt is invariant with decrease in b, the term δ^p/b increases without limit to the right as b approaches zero and the area approaches infinity. Thus, the fracture toughness of any material approaches infinity. This paradoxical situation calls for a natural limit to the reduction of b.

We recognize that only the material at the propagating crack tips is at its maximum extension, so that most of the material in the ligament length has not yet reached maximum extension. At some minimum ligament length b, however, all the material in the remaining cross section will be at maximum extension. At this point, unstable, rapid failure should ensue just as happens with fully extended unnotched specimens. The following relationship, analogous to an equation proposed by Thomas,[5] recognizes a minimum ligament length for stable propagation.

$$J_c = b_m W_f \tag{10}$$

where G is neglected (small compared with J), b_m is the smallest value of b for which stable crack growth is found, and W_f is the energy per unit volume to failure of an unnotched specimen of the same material. W_f is obviously identified with the bracketed term of eq. (9) at the onset of unstable crack growth.

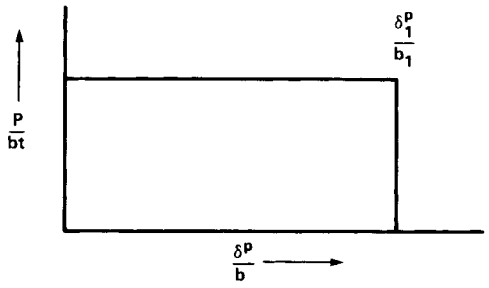

Fig. 3. Load per unit remaining area of unseparated material in the notch plane (net average stress) as a function of the ratio of plastic displacement to remaining ligament length (net stress assumed constant).

J_c is the *maximum possible fracture toughness allowable under plane stress and at specified rate and temperature.* J_c is always greater than J_{ic}, the fracture toughness at crack initiation. For brittle materials, J_c may be just slightly larger than J_{ic}. For sharp-tipped notches in ductile materials, J_c may be orders of magnitude larger than J_{ic}.

To show that eq. (10) has predictive value, it is necessary to show (1) that plots of P/tb vs. δ^p/b are independent of the starting and current ligament lengths (regardless of the particular shape of the envelope) and (2) that no values of $2\int(P/bt)d(\delta^p/b) - P\delta_1^p/b_1^2t$ exceed W_f.

The experiments described in the balance of this report are encouraging though not conclusive in supporting the proposed model of crack propagation.

It was convenient to work with high-density polyethylene sheets because the cracks propagated quite slowly through the ligament length. Under our rather elementary experimental procedures, the load and the remaining ligament length could be experimentally associated. This was seldom possible with the more rapid rates of crack growth that are found with more brittle plastics. Another factor encouraging the use of polyethylene was the necessity of measuring ligament thickness concurrently with the load and ligament-length measurements. Broad necked-down surfaces were available for thickness measurement.

EXPERIMENTAL

Specimens were 1-in.-wide dog-bone specimens described previously[6] and notched symmetrically on each side. The specimens were inked in a grid pattern extending to 0.5 in. above and below the notch plane. The specimens were pulled in an Instron testing machine. The grid pattern was photographed periodically to measure displacement across the plastic zone. An event marker was depressed simultaneously with the taking of the photograph to correlate displacement with load. In some cases, the thickness was obtained by measurement with a micrometer immediately after the photography.

Material

High-density polyethylene sheets of 0.02 g/10 min melt index (ASTM D1238, Condition E) were used. The sheets had an average thickness of 70 mils.

Experimental Analysis

Three quantities were measured on the negatives that were obtained by photographing the gridded zones of the specimens during extension: the total length of the grid zone in the direction of loading, the length of a zone from one end of the grid to a crossline just at the boundary of the yielded zone, and the distance between the notch tips.

Figure 4 shows a tracing of the load-displacement chart for run no. 4 with the polyethylene. The curve is highly nonlinear, the material exhibits considerable ductility, and the yield maximum is broad. The pips along the curve indicate the displacement at which photographs were taken. When tearing commenced, there was a steady drop in load. Figure 5 comprises photographs taken at various stages of the displacement, with the numbers corresponding to the numbered

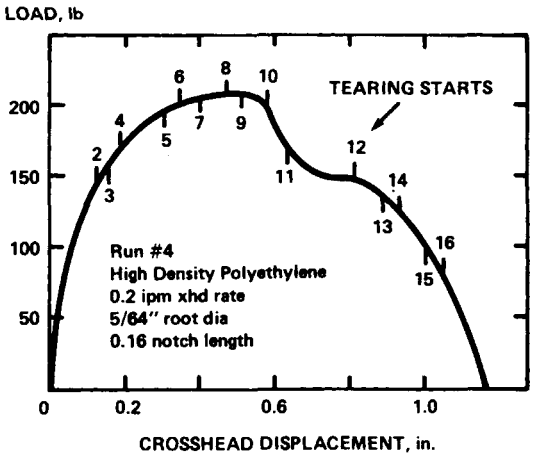

Fig. 4. Experimental load-total displacement trace of high density polyethylene. Pips on the trace represent points at which photographs were taken.

pips on Figure 4. The first frame was taken when the specimen was under zero load. Frame 9 represents the specimen at maximum load when yielding and necking had proceeded completely across the ligament length. Note that the width reduction of the grid is less in the notch plane than away from the notch plane. The through-thickness yielding occurs under nearly plane-strain conditions in the notch plane and develops and extends with increase in displacement. The notches become blunter, and finally tears start at each notch tip.

The example shown is one of the most misaligned crackgrowth patterns observed. Nonetheless, b was measured as indicated. As soon as the notch tips reached the same vertical plane, complete separation occurred along a fraction in the vertical plane. The elastic component of the displacement was determined by measuring the distance l^e in the photograph. l^e was corrected to the total grid length by dividing l^e by its fraction of the total grid length at commencement of loading. Further mention of l^e is to be taken as "corrected" l^e. The total grid length l^t in the same vertical plane was also measured. Then

$$\begin{aligned} \delta^e &= l^e - l_0^e \\ \delta^t &= l^t - l_0^t \\ \delta^p &= \delta^t - \delta^e \end{aligned} \tag{11}$$

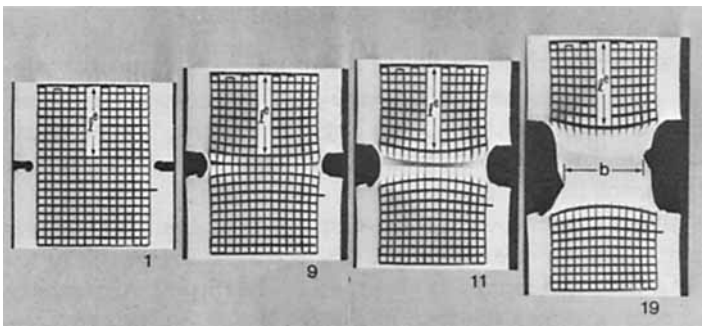

Fig. 5. Photographs of the inked grid on the specimen surface during displacement. Same specimen as Figure 4. Numbers correspond to the trace pip numbers in Figure 4.

where the subscript 0 refers to the measurement at commencement of loading. δ^e contains elastic components δ^c "due to the notch" and δ^{nc} "as if the notch were not present." δ^p is the plastic displacement "due to the notch." Because of the assumption of linear elastic displacement in the regions of the specimen away from the notch region, there is no δ^p as if the notch were not present. Therefore, because only δ^p is used in the subsequent calculations, it is not necessary to be concerned about the loading compliance.

The displacement and ligament-length readings were made on the negatives with an optical comparator to ensure precision. Table I contains two examples of the experimental readings and the resultant calculations. Only for runs at 0.002-ipm crosshead speed was it possible to obtain thickness readings with the present methods. It may be noted that the estimated δ^e often exceeds δ^t before the onset of full plastic yielding in the ligament, probably an artifact of the correction procedure. Also, note that crack initiation is not necessarily associated with maximum load.

Elongation to failure of an unnotched specimen of the material was required in order to measure W_f, the energy per unit volume, to failure of an unnotched specimen. A small tension-test specimen was photogridded, and photographs were taken periodically during the extension. On the photographs, the separation of two adjacent lines normal to the direction of extension was measured. Assuming a Poisson's ratio of $\frac{1}{2}$, the corresponding change in cross-sectional area was calculated. The true-stress–true-strain plot in Figure 6 was made where true strain was calculated as the natural logarithm of the elongation. The work per unit volume to failure was taken as the area under this curve and was determined to be 1.93×10^8 Pa.

RESULTS AND DISCUSSION

The results of the experiments at 0.2-ipm and 0.002-ipm crosshead speeds are displayed in Figure 7. The effects of thickness reduction are ignored, and the load per unit ligament width is plotted vs. the ratio of plastic displacement to ligament width. The tearing profile was blunter (the crack opening angle was larger) with the slower extension. This phenomenon is shown in Figure 8.

Repeated runs at 0.2-ipm crosshead speed for initial notch lengths from 0.08 to 0.32 in. and notch root diameters of $\frac{3}{64}$ to $\frac{7}{64}$ in. show reasonably good su-

TABLE I(a)
Calculation of Load and Plastic Displacements; Run No. 9, High-Density Polyethylene[a]

Frame no.	p (lb.)	b (in.)	P/b (lb/in.)	δ^e (in.)	δ^t (in.)	δ^p (in.)	δ^p/b
1	0	0.453	0	0	0	0	0
2	120	0.456	264	0.043	0.035	0	0
3	134	0.452	297	0.057	0.054	0	0
4	135	0.439	308	0.074	0.080	0.006	0.014
5	112	0.417	269	0.075	0.121	0.046	0.110
6	102	0.406	250	0.075	0.153	0.078	0.192
7	95	0.395	240	0.072	0.200	0.128	0.324
8	94	0.370	253	0.074	0.286	0.212	0.573
9	88	0.342	256	0.075	0.351	0.276	0.807
10	59	0.209	283	0.074	0.475	0.401	1.919

[a] Crack initiated after Frame 7. $\frac{5}{64}$-in. root diameter, 0.2-ipm crosshead speed.

TABLE I(b)
Calculation of Load and Displacement; Run No. 14, High-Density Polyethylene[a]

Frame no.	P (lb)	b (in.)	t (in.)	P/b (lb/in.)	P/tb (10^3 psi)	δ^e (in.)	δ^t (in.)	δ^p (in.)	δ^p/b
1	0	0.702	0.072	0		0	0	0	0
2	32	0.702		45		0.008	0.005	0	0
3	58	0.703		82		0.014	0.012	0	0
4	75	0.702		107		0.025	0.022	0	0
5	87	0.700		124		0.030	0.027	0	0
6	96	0.695		138		0.037	0.033	0	0
7	103	0.695		148		0.037	0.037	0	0
8	109	0.692		158		0.053	0.048	0	0
9	115	0.687		167		0.066	0.060	0	0
10	118	0.684		173		0.073	0.067	0	0
11	121	0.678		178		0.085	0.079	0	0
12	125	0.670		185		0.105	0.098	0	0
13	125	0.660		189		0.127	0.119	0	0
14	125	0.650		192		0.143	0.136	0	0
15	122	0.629		194		0.145	0.175	0.030	0.048
16	116	0.606		191		0.202	0.16	0.014	0.023
17	107	0.582		184		0.216	0.260	0.044	0.076
18	101	0.571		177		0.216	0.281	0.065	0.114
19	94	0.563		167		0.215	0.308	0.093	0.165
20	89	0.548		162		0.213	0.335	0.122	0.223
21	85	0.531		160		0.210	0.366	0.156	0.294
22	82	0.517	0.016	159	9.9	0.209	0.401	0.192	0.371
23	89	0.485	0.015	165	11.0	0.207	0.438	0.231	0.76
24	78	0.468	0.013	167	12.8	0.207	0.471	0.264	0.564
25	76	0.453	0.013	168	12.9	0.205	0.503	0.298	0.658
26	75	0.444	0.0125	169	13.5	0.205	0.523	0.318	0.716
27	74	0.426	0.013	174	13.4	0.206	0.562	0.356	0.836
28	73	0.410	0.013	178	13.7	0.205	0.595	0.386	0.941
29	70	0.388	0.012	180	15.0	0.206	0.638	0.432	1.113
30	69	0.378	0.012	183	15.2	0.204	0.666	0.462	1.222
31	68	0.372	0.012	183	15.3	0.207	0.693	0.486	1.306
32	68	0.367	0.012	185	15.4	0.205	0.704	0.499	1.360

[a] Crack initiation after Frame 17. $^3/_{64}$-in. root diameter, 0.002-ipm crosshead speed.

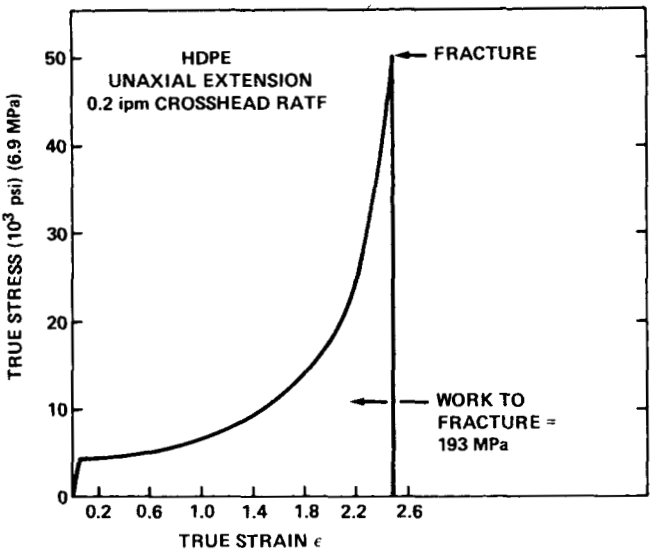

Fig. 6. True-stress–true-strain curve to failure of the high-density polyethylene used in this study.

perposition in Figure 7. The plot is independent of ligament length. The position on the abscissa depends only on the current value of ligament length regardless of the initial value even if cracks are propagating from the notch root. For the lower rate of crosshead displacement, the curve profile remains similar but is shifted vertically downward for 0.002 ipm to about 75% of its value at 0.2 ipm.

Data on thickness reduction at the slow rate were available so that it is possible to calculate the quantity P/bt and plot that against δ_p/b. This plot is shown in Figure 9, and the two sets of data are probably overlapping and part of a continuous curve. The y intercept is about 4 ksi and is deduced from the known

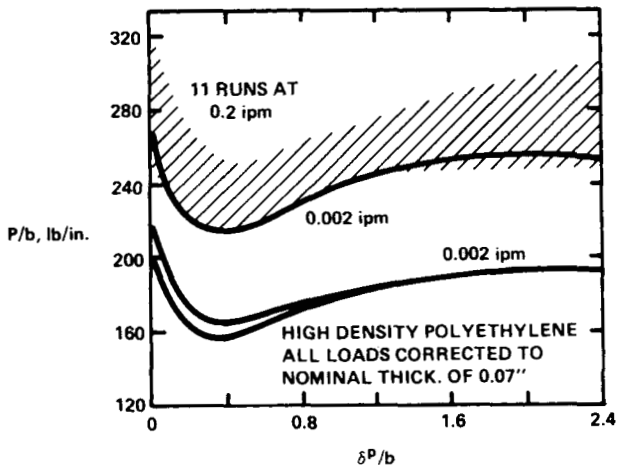

Fig. 7. Load (per unit remaining ligament length) as a function of the ratio of plastic displacement to remaining ligament length. Solid lines represent runs at 0.002 ipm. The shaded area encompasses the 11 runs at 0.2 ipm.

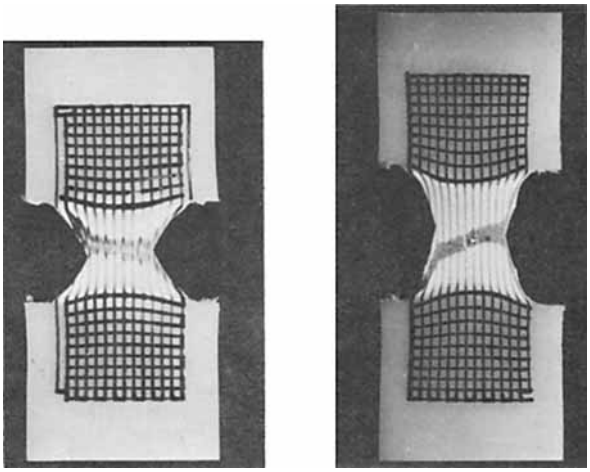

Fig. 8. The propagating crack operating angle is greater at the lower crosshead speed.

yield strength of this material. A continuous line has been drawn through the points.

Because the area under the curve is simply related to the bracketted factor of eq. (9), J is calculated by determining the area under the curve to a given remaining ligament length, calculating the bracketed factor, and multiplying it by the remaining ligament length. There are two points of elaboration to be made on the basis of the results expressed in Figure 9.

The first is the question of how large an area is the maximum allowable. It was said in the Introduction that this was given by

$$J_c = b_m W_f \tag{10}$$

and therefore

$$2(\text{area}) - \frac{P\delta^P}{b^2 t} \leq W_f \tag{12}$$

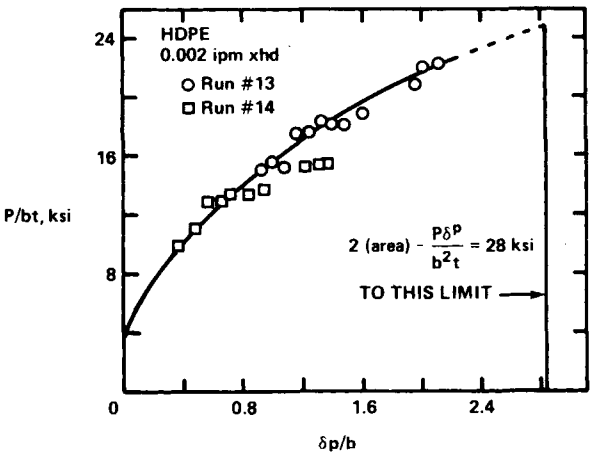

Fig. 9. Net average notch plane stress as a function of the ratio of the plastic displacement to remaining ligament length. The limiting area to the vertical solid line is calculated by eq. (10) using the data of Figure 6 to define the limiting area.

TABLE II
Calculation of Fracture Toughness J from Load Curve Area Measurements

δ^p/b	Area (psi)	$p\delta^p/b^2t$ (psi)	2 (area) − $p\delta^p/b^2t$	b_1 (in.)	J (lb/in.)
0.2	1136	1440	830		
0.4	2912	4000	1820	0.52	950
0.6	5120	6960	3280	0.46	1510
0.8	7710	10,880	4540	0.43	1950
1.0	10,620	15,200	6050	0.40	2420
1.2	13,860	20,160	7550	0.38	2870
1.4	17,340	25,200	9490		
1.6	21,100	31,400	10,850		
1.8	25,100	37,400	12,700		
2.0	29,300	43,200	15,460		
2.2	33,700	49,300	18,180		
2.4	38,300	55,700	20,900		
2.6	43,000	62,400	23,600		
2.8	47,900	68,300	27,500		

If we obtain points on the curve such that eq. (12) is violated, the conjecture is wrong. Our sparse data fall within the bounds. There is a question of the application of W_f to the notched specimen because the data were obtained at a 0.2-ipm crosshead rate for the unnotched specimen and at a 0.002-ipm crosshead rate for the notched specimen. This difference is not as large as it appears because the different effective gage lengths will reduce the effective difference. Another mitigating factor is the rapid rise in the left side of eq. (12) as the 28 ksi limit is approached. Thus, a downward shift of W_f will not move the limit to the left very drastically.

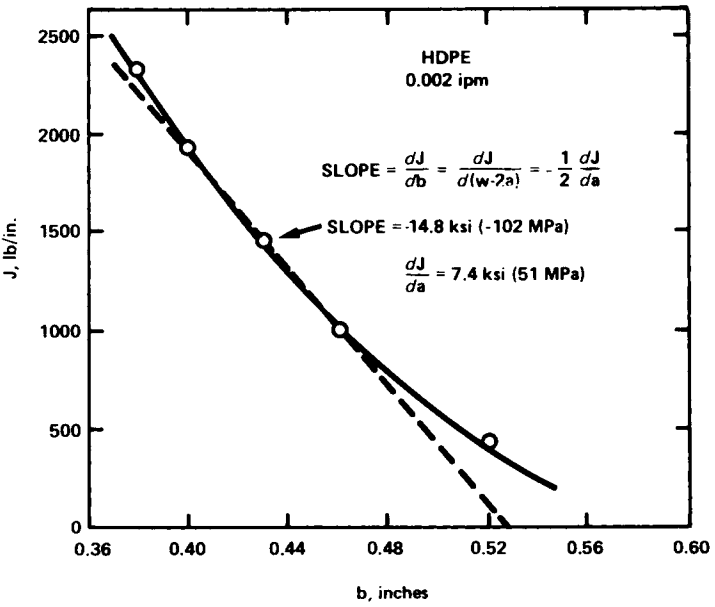

Fig. 10. Increase in J during the crack growth phase. The tangent to the curve gives the change in J per unit change in crack length. dJ/da is predicted to reach a limiting value of 56 ksi (385 MPa) ultimate slope prior to complete specimen failure.

The second point is that the ability to calculate $\Delta J/\Delta a$ from this data can be demonstrated. In Table II, the calculation of J from the data of run no. 14 is demonstrated. Then J is plotted versus the remaining ligament length (Fig. 10). The slope of this curve is related to $\Delta J/\Delta a$ as indicated. At a ligament length of 0.43 in., $\Delta J/\Delta a$ has a value of 29.6 ksi and is increasing as b decreases. From eq. (10), we predict that unstable fracture occurs when $\Delta J/\Delta a > 56$ ksi. The reader should note the close resemblance of these results with results for ductile metals reported by Paris et al.[7] and Hutchinson and Paris.[8]

It is to be noted parenthetically that instability onset can occur not only by material instability as detailed above but also by load compliance and thermal instability.[9]

CONCLUSIONS

1. The Burns–McMeeking equation forms an efficient mechanism to plot crack-growth data on a universal plot that is independent of geometry.
2. High-density polyethylene yields crack-growth data for double-edge-notched specimens in tension that follow the predicted form of Burns and McMeeking.
3. Consideration of the limits of material extension leads to a prediction of a material instability threshold for ductile crack growth.
4. Limited experimental data support the concept of a material-instability threshold.

References

1. J. R. Rice, P. C. Paris, and J. C. Merkel, ASTM STP 536, Philadelphia, 1974, pp. 231–245.
2. J. A. Begley, W. A. Logsdon, and J. D. Landes, ASTM STP 631, Philadelphia, 1977, pp. 112–120.
3. W. F. Brown, Jr., and J. E. Srawley, "Plane Strain Crack Toughness of High Strength Metallic Materials," STP 410, American Society for Testing and Materials, Philadelphia, 1966.
4. S. J. Burns and R. M. McMeeking, *Int. J. Fracture*, **14**, R73–R76 (1978).
5. A. G. Thomas, *J. Polym. Sci.*, **18**, 177–188 (1955).
6. R. D. Hoffman, Society of Plastic Engineers 37th Annual Technical Conference Preprints, 1979, pp. 537–545.
7. P. C. Paris, H. Tada, A. Zahoor, and H. Ernst, ASTM STP 688, Philadelphia, 1979, pp. 5–36.
8. J. W. Hutchinson and P. C. Paris, ASTM STP 668, Philadelphia, 1979, pp. 37–64.
9. E. J. Kramer, *J. Appl. Polym. Sci.*, **14**, 2825–2832 (1970).

Received June 12, 1981
Accepted December 10, 1981